PERGAMON

Available online at www.sciencedirect.com
SCIENCE DIRECT®

Polyhedron 22 (2003) 109–118

POLYHEDRON

www.elsevier.com/locate/poly

Nitrosyl-cobalt monocarbollide complexes

Jason A. Kautz, Thomas D. McGrath, F. Gordon A. Stone *

Department of Chemistry and Biochemistry, Baylor University, Waco, TX 76798-7348, USA

Received 12 July 2002; accepted 19 August 2002

Abstract

The carborane anion [*closo*-2-$CB_{10}H_{11}$]$^-$ undergoes a polyhedral expansion reaction with [$Co(CO)_3(NO)$] in tetrahydrofuran (THF) to afford [2-CO-2-NO-*closo*-2,1-$CoCB_{10}H_{11}$]$^-$, isolated as the [$N(PPh_3)_2$]$^+$ salt **1a**. An X-ray diffraction study confirmed that the NO group is linearly bonded to cobalt. The CO ligand in **1a** is readily replaced by PPh_3 in the presence of Me_3NO, or by PEt_3 or CNBu^t directly, to give the species [$N(PPh_3)_2$][2-L-2-NO-*closo*-2,1-$CoCB_{10}H_{11}$] [L = PPh_3 (**1b**), PEt_3 (**1c**), CNBu^t (**1d**)]. Reactions of these anionic complexes with electrophilic reagents are exemplified by treatment of **1c** with CF_3SO_3Me in CH_2Cl_2–THF to give the neutral, zwitterionic *B*-THF species [2-NO-2-PEt_3-7-$O(CH_2)_4$-*closo*-2,1-$CoCB_{10}H_{10}$] (**3a**), and by the reaction of **1b** with [$CuCl(PPh_3)]_4$ and Tl[PF_6] in THF to give bimetallic [2,7,11-{$Cu(PPh_3)$}-7,11-(μ-H)$_2$-2-NO-2-PPh_3-*closo*-2,1-$CoCB_{10}H_9$] (**4b**). X-ray diffraction analysis of crystals of **4b** confirmed the presence of a Co–Cu bond.

Keywords: Cobalt complexes; Nitrosyl ligands; Crystal structures; Carborane ligands

---

1. Introduction

The discovery almost 40 years ago that the dicarbollide ligand [*nido*-7,8-$C_2B_9H_{11}$]$^{2-}$ could form π complexes with transition metals initiated the area of carbametallaborane chemistry [1]. Not long thereafter, it was shown that the monocarbollide ligand [*nido*-7-$CB_{10}H_{11}$]$^{3-}$ had similar ligating properties [2] with, in addition, a higher negative charge that could potentially lead to differences in behavior. Like the isolobal cyclopentadienide ligand [C_5H_5]$^-$, these di- and monocarbollide ligands behave as pentahapto, 6π-electron donors to transition element centers. However, whereas the cyclopentadienide group has played a central role in the development of modern organometallic chemistry [3], the corresponding carbollide species have been far less extensively studied, and this is particularly so for the monocarbon species [4]. As part of a program which begins to redress this imbalance we are preparing and studying the reactivity of several 'piano stool'-type complexes in which a metal center is bonded on one side by a monocarbollide ligand and on the other by CO groups, the latter often in combination with isocyanides or phosphines [5–14].

To date, the parent species [2,2,2,2-$(CO)_4$-*closo*-2,1-$MCB_{10}H_{11}$]$^-$ (M = Mo [8], W [12]), [2,2,2-$(CO)_3$-*closo*-2,1-$ReCB_{10}H_{11}$]$^{2-}$ [6], [2,2,2-$(CO)_3$-*closo*-2,1-$MCB_{10}H_{11}$]$^-$ (M = Fe [8], Ru [10], Os [10]) and [2,2-$(CO)_2$-*closo*-2,1-$NiCB_{10}H_{11}$]$^-$ [14] have all been reported. Notable by their absence from this list are representative complexes of the Group 9 metals, of which the cobalt complex [2,2-$(CO)_2$-*closo*-2,1-$CoCB_{10}H_{11}$]$^{2-}$ would be a reasonable target. Thus far attempts to obtain this or similar species by the routes that successfully gave the above related complexes have been unsuccessful. Moreover, although a dimeric complex of Co^{II} was obtained from [$Co_2(CO)_8$] and the dicarborane [*nido*-7,8-$C_2B_9H_{13}$] [15], neither the analogous monocarbollide species [2,*B*′-μ-H-2-CO-*closo*-2,1-$CoCB_{10}H_{10}$]$_2^{2-}$, nor any other identifiable products, was obtained from the ostensibly parallel reaction between the same cobalt reagent and [*nido*-7-$CB_{10}H_{13}$]$^-$. However, we here report upon the synthesis and reactivity of a nitrosyl cobalt-monocarbollide complex that is closely related to the originally targeted dicarbonyl species. These products are members of the rare class of nitrosyl-substituted metallacarboranes [16].

---

* Corresponding author. Tel.: +1-254-710-4427; fax: +1-254-710-2403

E-mail address: gordon_stone@baylor.edu (F.G.A. Stone).

0277-5387/02/$ - see front matter © 2002 Elsevier Science Ltd. All rights reserved.
PII: S0277-5387(02)01261-5

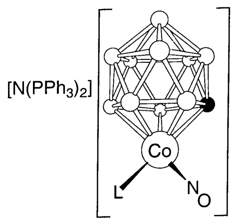

	L
1a	CO
1b	PPh$_3$
1c	PEt$_3$
1d	CNBu^t

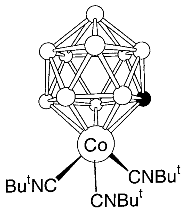

2

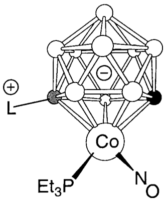

	L
3a	O(CH$_2$)$_4$
3b	NCMe
3c	N(Me)=C(H)Me

○ BH ◍ B ● C

2. Discussion

Almost 30 years ago, it was discovered that zerovalent d^{10} metal centers could oxidatively insert into *closo*-carboranes, the resulting net two-electron transfer opening the cluster to afford a *nido*-carborane ligand which complexed with the divalent metal fragment formed [17]. This 'polyhedral expansion' approach was successfully used in the reaction of Ni^0 reagents with [*closo*-2-CB$_{10}$H$_{11}$]$^-$ to give species with a {*closo*-2,1-NiCB$_{10}$} architecture [18]. Since the cobalt center in the reagent [Co(CO)$_3$(NO)] may also be considered as of d^{10} configuration we surmised that it might act as a source of the {Co(CO)(NO)}$^{2+}$ fragment, isoelectronic with {Co(CO)$_2$}$^+$ and {Ni(CO)$_2$}$^{2+}$, in a similar oxidative insertion reaction.

Accordingly, [NMe$_4$][*closo*-2-CB$_{10}$H$_{11}$] was treated with [Co(CO)$_3$(NO)] in THF. After addition of [N(PPh$_3$)$_2$]Cl and column chromatography, the desired product [N(PPh$_3$)$_2$][2-CO-2-NO-*closo*-2,1-CoCB$_{10}$H$_{11}$] (**1a**) was obtained in reasonable yield. A second, unstable product may also be isolated in low variable yield from the reaction. This species readily decomposes to give **1a** and other unidentified compounds. Thus far, its instability has hindered its full characterization. However, its infrared spectrum (CH$_2$Cl$_2$) shows two CO (ν_{max} 2018 vs, 1979 s cm^{-1}) and two NO (ν_{max} 1811 s, 1768 vs cm^{-1}) stretching bands in addition to a broad band for BH stretches, and on that basis this compound is believed to be a dicobalt-carborane species. We hope to report more fully upon this product in the future.

Compound **1a** is characterized by the data given in Tables 1–3. The IR stretching frequencies (CH$_2$Cl$_2$) for the carbonyl (ν_{max} 2044 s cm^{-1}) and nitrosyl (ν_{max} 1807 s cm^{-1}) groups are within the expected ranges. In the compound's ^{1}H NMR spectrum, the cage CH group gives rise to a broad resonance at δ 2.28, with a corresponding broad signal in the ^{13}C{^{1}H} NMR spectrum at δ 46.7. The latter spectrum also shows a broad peak for the cobalt-bound CO group at δ 208.6. In the ^{11}B{^{1}H} NMR spectrum, the observation of a 1:2:2:1:2:2 intensity pattern is consistent with the retention of mirror symmetry within the anion, as anticipated.

Although these data reasonably confirmed compound **1a** to be the product expected, an X-ray diffraction analysis was performed in order to establish this definitively and to examine for any structural novelty in the anion. The result of the structure determination is shown in Fig. 1, along with selected geometric parameters. This study reveals the anion of **1a** to be of conventional, icosahedrally-based geometry: the cobalt center on one side is pentahapto-coordinated by the $\overline{\text{CBBBB}}$ face of the *nido*-carborane ligand, and on the other side is bonded to linear CO and NO groups [Co–C(2)–O(2) = 174.0(7)°; Co–N(1)–O(1) = 176.0(7)°]. Within the carbonyl and nitrosyl ligands, the internal distances [1.134(8) and 1.166(7) Å, respectively] are quite normal. The cobalt-to-cage bonding distance is approximately equivalent for all five atoms of the open carborane face [Co–CB$_4$ range 2.104(8)–2.177(7) Å], with no significant lateral 'slippage' [19] of the metal with respect to the cage carbon atom.

Upon addition of stronger donor ligands L, the CO rather than the NO in **1a** is preferentially replaced. Thus, with L = PPh$_3$, PEt$_3$ or CNBu^t in CH$_2$Cl$_2$ solutions, **1a** is converted to the purple compounds [N(PPh$_3$)$_2$][2-L-2-NO-*closo*-2,1-CoCB$_{10}$H$_{11}$] [L = PPh$_3$ (**1b**), PEt$_3$ (**1c**), CNBu^t (**1d**)]. The yield of **1b** is significantly improved, and the reaction time reduced, by addition of Me$_3$NO to remove the CO as CO$_2$. Data characterizing complexes **1b**–**1d** are listed in Tables 1–3. All three compounds in their ^{11}B{^{1}H} NMR spectra display the same symmetrical pattern of resonances as **1a** (with some coincidences), with a slight overall shift to higher field consistent with the increased cluster electron density originating from the added donors L. Correspondingly, their cage CH units resonate at δ 1.37 (**1b**), 1.66 (**1c**) and 1.97 (**1d**) in their ^{1}H NMR spectra, also to higher field than in the precursor **1a**. The same units likewise show broad signals in their ^{13}C{^{1}H} NMR spectra, at δ 47.3 (**1b**), 44.3 (**1c**) and 45.7 (**1d**), close to that observed in the spectrum of **1a**. The ligands L themselves also give rise to peaks in the ^{1}H, ^{13}C{^{1}H} and ^{31}P{^{1}H} NMR spectra, in typical positions. All of the compounds **1** are reasonably air stable as solids, but suffer from thermal instability. The latter is somewhat ameliorated by the presence of the donors L in **1b**–**1d**.

Table 1
Analytical and physical data

Compound	Color	Yield (%)	ν_{max}(NO) (cm^{-1}) [a]	Analysis (%) [b]		
				C	H	N
[N(PPh$_3$)$_2$][2-CO-2-NO-*closo*-2,1-CoCB$_{10}$H$_{11}$] (**1a**)	brown	60	1807 s [c]	58.0 (58.0)	5.3 (5.2)	3.5 (3.6)
[N(PPh$_3$)$_2$][2-NO-2-PPh$_3$-*closo*-2,1-CoCB$_{10}$H$_{11}$] (**1b**)	purple	62	1765 s	60.6 (60.8) [d]	5.3 (5.3)	2.6 (2.5)
[N(PPh$_3$)$_2$][2-NO-2-PEt$_3$-*closo*-2,1-CoCB$_{10}$H$_{11}$] (**1c**)	purple	81	1752 s	59.0 (58.9)	6.4 (6.4)	3.3 (3.2)
[N(PPh$_3$)$_2$][2-CNBu^t-2-NO-*closo*-2,1-CoCB$_{10}$H$_{11}$] (**1d**)	purple	70	1774 s [e]	58.8 (58.8) [f]	6.0 (5.9)	5.0 (4.9)
[2,2,2-(CNBu^t)$_3$-*closo*-2,1-CoCB$_{10}$H$_{11}$] (**2**)	yellow	69	[g]	43.6 (43.7)	8.6 (8.7)	9.4 (9.6)
[2-NO-2-PEt$_3$-7-O(CH$_2$)$_4$-*closo*-2,1-CoCB$_{10}$H$_{10}$] (**3a**)	purple	40	1770 s	32.2 (32.3)	8.0 (8.1)	3.2 (3.4)
[2-NO-2-PEt$_3$-7-NCMe-*closo*-2,1-CoCB$_{10}$H$_{10}$] (**3b**)	purple	36	1772 s	31.7 (31.1) [h]	7.2 (7.9)	6.4 (7.1)
[2,7,11-{Cu(PPh$_3$)}-7,11-(μ-H)$_2$-2-NO-2-PPh$_3$-*closo*-2,1-CoCB$_{10}$H$_9$] (**4b**)	purple	91	1812 m	54.9 (55.0)	5.1 (5.1)	1.8 (1.7)
[2,7-{Ag(PPh$_3$)}-7-μ-H-2-NO-2-PPh$_3$-*closo*-2,1-CoCB$_{10}$H$_{10}$] (**5**)	purple	78	1808 m	51.3 (51.2) [f]	4.8 (4.8)	1.6 (1.6)
[2-{Au(PPh$_3$)}-2-NO-2-PPh$_3$-*closo*-2,1-CoCB$_{10}$H$_{11}$] (**6**)	brown–purple	10	1818 m	48.5 (48.5) [i]	5.1 (4.9)	1.6 (1.4)

[a] Measured in CH$_2$Cl$_2$; a broad, medium-intensity band observed at ca. 2500–2550 cm^{-1} in the spectra of all compounds is due to B–H absorptions.
[b] Calculated values are given in parentheses.
[c] ν_{max}(CO) 2044 s cm^{-1}.
[d] Crystallizes with 1 mol. equiv. of CH$_2$Cl$_2$.
[e] ν_{max}(NC) 2169 m cm^{-1}.
[f] Crystallizes with 0.25 mol. equiv. of CH$_2$Cl$_2$.
[g] ν_{max}(NC) 2207 s, 2184 s cm^{-1}.
[h] Crystallizes with 0.25 mol. equiv. of pentane.
[i] Crystallizes with 0.5 mol. equiv. of pentane.

However, all four species can survive for many months under N$_2$ at −30 °C.

During the synthesis of compound **1d**, a second cobalt–carborane complex was on occasion also observed to form in very low yield. Initial infrared spectroscopic analysis (Table 1) indicated the NO group was absent and instead two NC stretching bands (ν_{max} 2207 s, 2184 s cm^{-1}) are seen. This yellow product was

Table 2
^{1}H and ^{13}C NMR data [a]

Compound	^{1}H/δ [b]	^{13}C/δ [c]
1a	7.68–7.46 (m, 30H, Ph), 2.28 (br s, 1H, cage CH)	208.6 (br, CO), 136.2–126.8 (Ph), 46.7 (br, cage C)
1b	7.68–7.36 (m, 45H, Ph), 1.37 (br s, 1H, cage CH)	134.8–126.6 (Ph), 47.3 (br, cage C)
1c	7.66–7.46 (m, 30H, Ph), 2.00 [dq, 6H, PC*H$_2$*, *J*(HH) = 8, *J*(PH) = 8], 1.66 (br s, 1H, cage CH), 1.15 [dt, 9H, PCH$_2$*Me*, *J*(HH) = 8, *J*(PH) = 16]	134.0–126.8 (Ph), 44.3 (br, cage C), 17.7 [d, P*C*H$_2$, *J*(PC) = 28], 8.3 [br d, PCH$_2$*Me*, *J*(PC) = 7]
1d	7.68–7.46 (m, 30H, Ph), 1.97 (br s, 1H, cage CH), 1.59 (s, 9H, Bu^t)	155.2 (br, CN), 136.3–126.7 (Ph), 58.3 (*C*Me$_3$), 45.7 (br, cage C), 30.4 (C*Me$_3$*)
2	2.15 (br s, 1H, cage CH), 1.53 (s, 27H, Bu^t)	144.3 (br, CN), 59.1 (*C*Me$_3$), 52.1 (br, cage C), 30.2 (C*Me$_3$*)
3a	4.42 (m, 4H, OCH$_2$), 2.26–2.05 (m, 10H, PCH$_2$ and OCH$_2$C*H$_2$*), 1.78 (br s, 1H, cage CH), 1.17 [dt, *J*(PH) = 16, *J*(HH) = 8, 9H, CH$_3$]	82.9 (OCH$_2$), 43.5 (br, cage C), 25.7 (OCH$_2$*C*H$_2$), 18.1 [d, *J*(PC) = 27, PCH$_2$], 9.4 (br, CH$_3$)
3b	2.66 (s, 3H, NCMe), 2.11 (br m, 6H, PCH$_2$), 1.89 (br s, 1H, cage CH), 1.18 [dt, *J*(PH) = 15, *J*(HH) = 8, 9H, PCH$_2$C*H$_3$*]	113.7 (NC), 46.6 (br, cage C), 18.2 [d, *J*(PC) = 29, PCH$_2$], 8.3 (br, PCH$_2$*C*H$_3$), 1.1 (NC*Me*)
3c	7.91 (br m, 1H, =CH), 3.68 (br m, 3H, =NMe), 2.54 [dq, ^{3}*J*(HH) = 6, ^{4}*J*(HH) = 1, 3H, =C(H)*Me*], 2.11 (br m, 6H, PCH$_2$), 1.81 (br s, 1H, cage CH), 1.15 [dt, *J*(PH) = 16, *J*(HH) = 8, 9H, PCH$_2$C*H$_3$*]	174.7 (N=C), 55.4 (NMe), 47.3 (br, cage C), 18.3 [=C(H)*Me*], 18.1 [d, *J*(PC) = 29, PCH$_2$], 8.5 (br, PCH$_2$*C*H$_3$)
4a	7.71–7.19 (m, 15H, Ph), 2.86 (br s, 1H, cage CH)	202.0 (br, CO), 135.0–129.0 (Ph), 56.9 (br, cage C)
4b	7.44–7.00 (m, 30H, Ph), 1.76 (br s, 1H, cage CH)	135.3–129.0 (Ph), 54.6 (br, cage C)
5	7.49–7.20 (m, 30H, Ph), 1.73 (br s, 1H, cage CH)	135.2–129.0 (Ph), 54.6 (br, cage C)
6	7.61–7.16 (m, 30H, Ph), 1.39 (br s, 1H, cage CH)	135.4–127.9 (Ph), 56.3 (br, cage C)

[a] Chemical shifts (δ) in ppm, coupling constants (*J*) in Hz, measurements at ambient temperatures in CD$_2$Cl$_2$.
[b] Resonances for terminal BH protons occur as broad unresolved signals in the range δ ca. −1 to +3.
[c] ^{1}H-decoupled chemical shifts are positive to high frequency of SiMe$_4$.

Table 3
^{11}B and ^{31}P NMR data [a]

Compound	$^{11}B/\delta$ [b]	$^{31}P/\delta$ [c]
1a	6.4, 2.3 (2B), −4.1 (2B), −5.2, −9.6 (2B), −16.9 (2B)	
1b	1.3 (3B), −5.5 (2B), −7.0, −12.6 (2B), −18.5 (2B)	49.3 (br)
1c	0.1 (3B), −6.8 (2B), ca. −7.3 (sh), −13.1 (2B), −18.8 (2B)	36.5 (br)
1d	2.1, 0.7 (2B), −5.9 (2B), −6.3, −11.9 (2B), −18.1 (2B)	
2	14.8, 2.3 (2B), −1.2 (2B), −5.4, −7.7 (2B), −14.1 (2B)	
3a	25.1 [B(7)], −2.1, −6.2, −8.0, −9.0, −10.5, −14.4, −15.6, −19.0, −23.2	37.9 (br)
3b	2.3 [B(7)], −1.1, −4.6, −6.3, −8.0, −8.9, −12.6, −13.9, −18.2, −19.6	38.8 (br)
3c	13.3 [B(7)], −1.5, −5.9, ca. −6.6 (sh), −7.9, −10.1, −11.9, −13.9, −18.0, −19.9	39.3 (br)
4a	10.6, −2.2 (2B), −8.0 (5B), −13.1 (2B)	9.6 (br)
4b	5.5, −3.2 (2B), −8.0, −9.6 (2B), −10.3 (2B), −14.7 (2B)	42.3 (br, $CoPPh_3$), 9.3 (br, $CuPPh_3$)
5	5.7, −3.4, −4.2, −8.0, −8.1, −9.0 (2B), −11.6, −13.9, −15.2	42.7 (br, $CoPPh_3$), ca. 18.5 (v br d, *J* ca. 700, $AgPPh_3$)
6	6.8, −2.8 (v br, 4B), −7.6 (2B), −8.7 (2B), −14.2	42.0 (br, $CoPPh_3$), 38.8 (br, $AuPPh_3$)

[a] Chemical shifts (δ) in ppm, coupling constants (J) in Hz, measurements at ambient temperatures in CD_2Cl_2.

[b] ^1H-decoupled chemical shifts are positive to high frequency of $BF_3\cdot Et_2O$ (external); resonances are of unit integral except where indicated.

[c] ^1H-decoupled chemical shifts are positive to high frequency of 85% H_3PO_4 (external). The compounds **1** additionally show a singlet at δ 21.7 for the $[N(PPh_3)_2]^+$ cation.

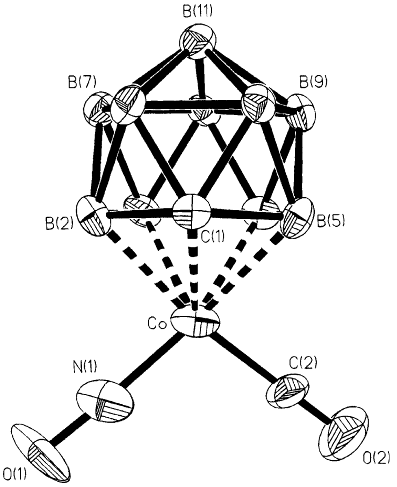

Fig. 1. Structure of the anion [2-CO-2-NO-*closo*-2,1-$CoCB_{10}H_{11}]^-$ in **1a**. Thermal ellipsoids are shown at the 40% probability level and hydrogen atoms are omitted for clarity. Selected bond distances (Å) and interbond angles (°) are: Co–N(1) 1.712(7), Co–C(2) 1.725(7), Co–B(2) 2.104(8), Co–B(5) 2.143(7), Co–B(4) 2.154(7), Co–C(1) 2.169(5), Co–B(3) 2.177(7), N(1)–O(1) 1.166(7), C(2)–O(2) 1.134(8); O(1)–N(1)–Co 176.0(7), O(2)–C(2)–Co 174.0(7), N(1)–Co–C(2) 101.4(3), N(1)–Co–B(2) 86.9(3), C(2)–Co–B(2) 171.6(3), N(1)–Co–B(5) 155.3(3), C(2)–Co–B(5) 88.6(3), N(1)–Co–B(4) 149.5(3), C(2)–Co–B(4) 88.5(3), N(1)–Co–C(1) 112.7(2), C(2)–Co–C(1) 126.1(3), N(1)–Co–B(3) 105.1(3), C(2)–Co–B(3) 126.7(3).

further identified by NMR spectroscopy (Tables 2 and 3) as the Co^{III} species [2,2,2-$(CNBu^t)_3$-*closo*-2,1-$CoCB_{10}H_{11}$] (**2**). Its $^{11}B\{^1H\}$ NMR spectrum shows six signals in the ratio 1:2:2:1:2:2, consistent with retention of overall molecular symmetry and the general deshielding of these peaks relative to compounds **1** is indicative of the higher metal oxidation state. In the ^1H NMR spectrum of **2** two peaks are seen, with relative integrals 1:27. The former broad signal, at δ 2.15, is assigned as the cage CH proton, and the latter signal (δ 1.53) is due the Bu^t protons of the three isocyanide ligands. Peaks for the $CNBu^t$ groups are also seen in typical positions in the $^{13}C\{^1H\}$ NMR spectrum with, in addition, a broad resonance at δ 52.1 for the cage C atom.

It was subsequently found that with an excess $CNBu^t$ the same product **2** could be obtained from **1a** in yields of almost 70%. It seems reasonable that in this reaction **1a** is first converted to **1d**, and it may be that further $CNBu^t$ then displaces NO^+ to give dianionic [2,2-$(CNBu^t)_2$-*closo*-2,1-$CoCB_{10}H_{11}]^{2-}$. Oxidation of the latter by the liberated nitrosonium cation, followed by coordination of a third isocyanide, would then yield the observed product. We have observed previously that metal coordination and subsequent oxidation is a convenient route to complexes of the ligand [*nido*-7-$CB_{10}H_{11}]^{3-}$ with metals in higher oxidation states [13]. In contrast, direct reactions between the carborane trianion and a high-valent metal complex are largely unsuccessful, as the latter generally is incompatible with the strongly reducing properties of the carborane. In the present system, the ‘internal’ oxidizing agent NO^+ in **1a** (and **1d**) might point to a more general route to high-valent metal–carborane complexes.

Anionic metallacarboranes like the compounds **1** are susceptible to reactions with electrophiles [20]. In particular, the cage B–H groups may undergo hydride abstraction (by H^+, Me^+, etc.) and subsequent boron substitution in the presence of suitable ligands, allowing functionalization of the carborane cage. The synthesis of **1c** in good yield, and the expected enhancement of the cluster B–H units’ hydridic character by its PEt_3 ligand, make that compound an ideal substrate for the study of selected representative reactions of these cobaltacarborane anions towards electrophiles. Thus, treatment of **1c** with CF_3SO_3Me in CH_2Cl_2–THF or CH_2Cl_2–NCMe solutions gave the neutral zwitterionic compounds [2-NO-2-PEt_3-7-L-*closo*-2,1-$CoCB_{10}H_{10}$], L = $O(CH_2)_4$ (**3a**) or L = NCMe (**3b**), respectively. In addition to **3b**, the latter reaction system also gave in very low yield the species [2-NO-2-PEt_3-7-N(Me)=C(H)Me-*closo*-2,1-$CoCB_{10}H_{10}$] (**3c**), identified spectroscopically. By analogy with other {MCB_{10}} systems, these compounds are reasonably assigned as the 7-substituted isomers; that is, the boron atom bearing the ligand L is in a β position with respect to the carbon atom in the $\overline{\mathrm{CB}BB\mathrm{B}}$ face that coordinates the cobalt center. The species **3** are characterized by the data listed in Tables 1–3.

All three complexes show an increased NO stretching frequency in their infrared spectra [ν_{max} 1770 (**3a**), 1772 (**3b**) and 1767 (**3c**) cm^{-1}] compared with the precursor **1c**. This is consistent with the expected formation of neutral complexes. Substitution at a boron vertex in compounds **3** is immediately apparent from their $^{11}B\{^1H\}$ NMR spectra, all three of which show ten separate resonances consistent with the carborane fragment now lacking mirror symmetry. In addition, one signal in each spectrum (at δ 25.1 for **3a**, δ 2.3 for **3b** and δ 13.3 for **3c**) is assigned as the substituted vertex B(7), since these peaks remain singlets in fully proton-coupled ^{11}B NMR spectra. These chemical shifts are quite typical for such cage boron atoms bearing ether [8,11–13], nitrile [11], or iminium [11,12] substituents.

In the ^1H and $^{13}C\{^1H\}$ NMR spectra of compounds **3**, the substituents L were readily identified. The THF group in **3a** gives rise to two multiplets, each of relative intensity 4H, at δ 4.42 and ca. 2.1 in the ^1H spectrum, with corresponding signals at δ 82.9 and 25.7 in the $^{13}C\{^1H\}$ NMR spectrum. For **3b**, the protons of the NCMe substituent resonate at δ 2.66, whilst its carbon atoms give peaks at δ 113.7 (NC) and 1.1 (Me). In the ^1H NMR spectrum of **3c**, the =CH and =NMe protons are seen as broad multiplets at δ 7.91 and 3.68, respectively, whilst the iminium *C*-methyl protons give rise to a doublet of quartets at δ 2.54. Correspondingly, the $^{13}C\{^1H\}$ NMR spectrum of **3c** shows a diagnostic signal at δ 174.7 for the iminium moiety, along with peaks at δ 55.4 and 18.3 for the N- and C-bound iminium methyl groups, respectively. On the basis of the NMR data alone, it is impossible to definitively establish whether **3c** contains an iminium substituent with an *E* or *Z* configuration. However, although the *E* stereochemistry would be the more stable one, and in related ferracarborane species the *E* isomer is the only one observed [11], both isomers are formed in analogous molybdenum and tungsten systems [12]. Indeed, it may be that the alternate isomer to **3c** is also formed in the present case, but in yields too low to be detected.

The formation in this instance of nitrile-substituted **3b** as the major product is noteworthy. Previously, we have observed that treatment of metal–monocarbollide anions with CF_3SO_3Me in the presence of NCMe generally produced species in which the substituted boron exclusively carried an imine ligand N(Me)=C(H)Me [11,12], as in **3c**. The latter is believed to arise from NCMe *N*-methylation to form a nitrilium cation $[MeN{\equiv}CMe]^+$, which in turn behaves as the hydride abstracting agent, giving an imine which then ligates the naked boron atom. In the present case, it may be that the B–H groups are sufficiently hydridic that they successfully compete with NCMe for reaction with Me^+ and the high concentration of NCMe as solvent then leads to coordination of the boron atom by the nitrile group. Alternatively, an altogether different reaction mechanism may operate in this system, such as methylation at cobalt, followed by MeH reductive elimination and NCMe coordination.

Anionic metallamonocarboranes are also known to react with cationic transition-metal moieties to give bimetallic species [5–7,9,10,21]. The cations $\{M(PPh_3)\}^+$ (M = Cu, Ag, Au), which are isolobal with the proton, are typical fragments introduced in this manner. Treatment in THF of the parent cobalt–monocarbollide species **1a** with $[CuCl(PPh_3)]_4$ in the presence of $Tl[PF_6]$ surprisingly gave a mixture of two bimetallic products. Infrared analysis of the product mixture indicated two separate NO bands, but only a single CO stretching band. Chromatographic separation gave two fractions, which were identified spectroscopically (Tables 1–3) as the species [2,7,11-{$Cu(PPh_3)$}-7,11-(μ-H)$_2$-2-L-2-NO-*closo*-2,1-$CoCB_{10}H_9$], L = CO (**4a**) and L = PPh_3 (**4b**), respectively. Unfortunately, **4a** could not be obtained in pure form, as it quite readily decomposed in solution to give **4b**. Evidently the exopolyhedral attachment of the $\{Cu(PPh_3)\}^+$ fragment labilizes the CO group in **4a**. This is mirrored in an increased CO stretching frequency for **4a** (ν_{max} = 2073 cm^{-1}) relative to **1a** (ν_{max} = 2044 cm^{-1}), corresponding to a decrease in Co→CO backbonding. The NO frequency in **4a** (ν_{max} = 1847 cm^{-1}) is similarly increased.

Compound **4b** could also be prepared more cleanly and directly, and in far superior yield, from **1b** with $[CuCl(PPh_3)]_4$ and $Tl[PF_6]$. Both of the compounds **4** show similar NMR spectroscopic properties. Thus, their $^{11}B\{^1H\}$ NMR spectra show resonances in an intensity pattern 1:2:1:2:2:2 (with some coincidences for **4a**), suggestive of a symmetric structure on the NMR time scale. A broad signal in the $^{31}P\{^1H\}$ NMR spectrum at δ 9.6 (**4a**) and 9.3 (**4b**) is assigned to the phosphine bound to the exopolyhedral copper center. In addition, resonances for the PPh_3 and CO groups and the carborane cage are seen in typical positions in the ^1H and $^{13}C\{^1H\}$ NMR spectra of both compounds. However, no peaks are seen in the ^1H NMR spectra that could be attributed to protons involved in the B–H$\rightharpoonup$

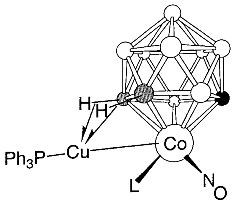

L

4a	CO
4b	PPh_3

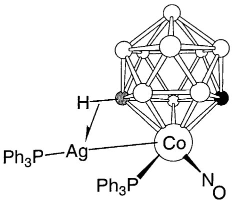

5

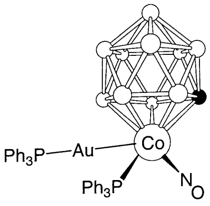

6

○ BH ◍ B ● C

Cu linkages that anchor the copper to the exopolyhedral surface. This is likely due to solution dynamic behavior whereby the copper fragment migrates over the cluster surface, a process that is fast on the NMR time scale [9].

The presence of a copper–cobalt bond in the compounds **4** was thought likely, by analogy with the known architecture of the copper–platinacarborane species [2,7,11-$\{Cu(PPh_3)\}$-7,11-(μ-H)$_2$-2,2-$(PEt_3)_2$-*closo*-2,1-$PtCB_{10}H_9$] which similarly contains a d^8 metal fragment incorporated into a $\{$*closo*-2,1-$MCB_{10}H_{11}\}$ cluster [5]. However, the corresponding $\{Cu(PPh_3)\}$ derivatives of the $\{$*closo*-2,1-$FeCB_{10}H_{11}\}$ and $\{$*closo*-2,1-$MoCB_{10}H_{11}\}$ clusters have no direct metal–copper bonds [9]. In the absence of any diagnostic information from the ^1H NMR data, therefore, an X-ray diffraction analysis was necessary in order to confirm the presence of the Co–Cu contacts. Suitable single crystals of **4b** were available and the molecular structure determined is shown in Fig. 2, together with selected bond distances and angles.

As expected, **4b** consists of a central $\{$*closo*-2,1-$CoCB_{10}H_{11}\}$ cluster that bears NO and PPh_3 ligands bound to the cobalt vertex [Co–N is 1.637(8) Å and Co–P(1) is 2.258(2) Å]. As in the parent species **1a**, the NO ligand is again essentially linear, with N–O(2) 1.160(8) Å and Co–N–O(2) 176.0(6)°. In addition, a $\{Cu(PPh_3)\}$ fragment is bonded exopolyhedrally to a CoB_2 triangular face via a Co–Cu bond [2.597(2) Å] and two three-center, two-electron B–H⇀Cu agostic-type linkages. The Cu–B(3) and Cu–B(4) distances are 2.146(9) and 2.193(9) Å, respectively. Although the H atoms that bridge between boron and copper were not located in the X-ray diffraction study, they were included in calculated positions since their presence is chemically sensible and is supported by the observation of proton coupling for all signals in the ^{11}B NMR spectrum.

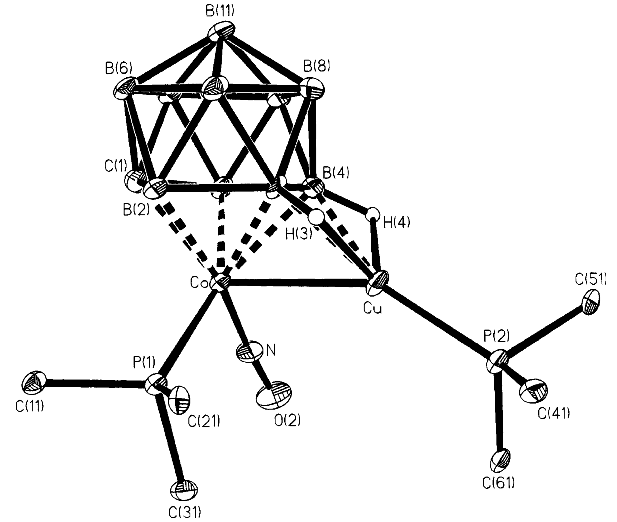

Fig. 2. Molecular structure of [2,7,11-$\{Cu(PPh_3)\}$-7,11-(μ-H)$_2$-2-NO-2-PPh_3-*closo*-2,1-$CoCB_{10}H_9$] (**4b**) in **4b**·OEt_2. Thermal ellipsoids are drawn with 40% probability and for clarity hydrogen atoms are omitted, except H(3) and H(4) which are shown as small circles of arbitrary radius. Selected bond distances (Å) and interbond angles (°) are: Co–N 1.637(8), Co–B(2) 2.112(9), Co–B(5) 2.126(10), Co–C(1) 2.144(7), Co–B(4) 2.148(8), Co–B(3) 2.167(10), Co–P(1) 2.258(2), Co–Cu 2.597(2), N–O(2) 1.160(8), Cu–P(2) 2.175(2), Cu–B(3) 2.146(9), Cu–B(4) 2.193(9); N–Co–C(1) 125.8(4), N–Co–P(1) 93.5(2), C(1)–Co–P(1) 111.3(2), N–Co–Cu 88.6(2), C(1)–Co–Cu 130.3(2), P(1)–Co–Cu 99.15(8), N–Co–B(3) 139.5(3), N–Co–B(4) 101.8(3), P(1)–Co–B(3) 103.0(3), P(1)–Co–B(4) 148.1(3), O(2)–N–Co 176.0(6), P(2)–Cu–Co 146.82(8), P(2)–Cu–B(3) 155.2(3), P(2)–Cu–B(4) 147.5(3).

Silver and gold analogues of compound **4b** were prepared similarly from **1b**. Thus, with $Ag[BF_4]$ and PPh_3 the purple compound [2,7-$\{Ag(PPh_3)\}$-7-μ-H-2-NO-2-PPh_3-*closo*-2,1-$CoCB_{10}H_{10}$] (**5**) was obtained; and with $[AuCl(PPh_3)]$ in the presence of $Tl[PF_6]$, brown–purple [2-$\{Au(PPh_3)\}$-2-NO-2-PPh_3-*closo*-2,1-$CoCB_{10}H_{11}$] (**6**) was isolated. Although single crystals of these two species suitable for an X-ray diffraction study were not available they are likely to have the structures shown, by analogy with other related species [5,9,21]. The silver atom in such species is generally only three-coordinate, and therefore, only a single B–H⇀Ag linkage is necessary; whereas the gold atom prefers linear coordination and so would only require bonds to cobalt and the phosphine.

Data characterizing compounds **5** and **6** are given in Tables 1–3. The gold derivative is rather unstable in solution and hence could only be isolated in low yield. Both compounds are otherwise quite similar to **4b**, as is to be expected. Again, the NO stretching frequency [$\nu_{max} = 1808$ (**5**), 1818 (**6**) cm^{-1}] is higher than in the precursor **1b**. In their ^1H, $^{13}C\{^1H\}$ and $^{31}P\{^1H\}$ NMR spectra, peaks are seen in typical positions for the PPh_3 groups and the cage CH units give rise to broad resonances at δ_H 1.73 (**5**) and 1.39 (**6**) and at δ_C 54.6 (**5**) and 56.3 (**6**). As with **4b**, no signals are visible in the ^1H NMR spectrum that could be attributed to the H atoms involved in the proposed B–H⇀Ag linkage. Again, this is likely due to fluxional processes that are faster than the NMR time scale. In their $^{11}B\{^1H\}$ NMR data, however, the two compounds differ markedly. That for compound **6** has an intensity pattern 1:4:2:2:1, which would be consistent with the anticipated molecular symmetry. The spectrum for **5**, on the other hand, shows ten separate resonances (with one coincidence), suggestive of an asymmetric structure. This is surprising: although the compound would lack symmetry in the solid state, the fluxional processes referred to earlier should lend the molecule a time-averaged symmetric structure in solution. It may be that this is precluded by the precise mechanism of these processes, and the asymmetry of the quasi-tetrahedral silver center.

3. Conclusion

A range of novel nitrosyl-containing cobalt–moncarbollide complexes have been prepared, starting from the synthesis of **1a** via the oxidative insertion of $[Co(CO)_3(NO)]$ into $[closo\text{-}2\text{-}CB_{10}H_{11}]^-$. The anionic PEt_3 derivative **1c** was shown to undergo typical cage substitution reactions with hydride abstracting agents in the presence of suitable ligands, whilst the PPh_3 analogue **1b** with appropriate metal cations formed bimetallic species with metal–cobalt bonds. An additional interesting feature in this system was the formation of the Co^{III} species **2** from **1a** and excess $CNBu^t$. In the latter reaction, the NO^+ moiety in the starting compound was suggested as the probable oxidizing agent and this observation points to a possible more general route to $\{MCB_{10}\}$ species in which the metal M is in a high oxidation state. The potential of this methodology is yet to be explored.

4. Experimental

4.1. General considerations

All reactions were carried out under an atmosphere of dry, oxygen-free nitrogen using Schlenk line techniques. Solvents were distilled from appropriate drying agents under nitrogen prior to use. Petroleum ether refers to that fraction of boiling point 40–60 °C. Chromatography columns (typically ca. 15 cm in length and ca. 2 cm in diameter) were packed with silica gel (Acros, 60–200 mesh). Preparative thin-layer chromatography (TLC) was performed on Uniplates (silica gel G, Analtech). NMR spectra were recorded at the following frequencies: ^1H 360.1, ^{13}C 90.6, ^{31}P 145.8 and ^{11}B 115.5 MHz. The compounds $[NMe_4][closo\text{-}2\text{-}CB_{10}H_{11}]$ [22], $[CuCl(PPh_3)]_4$ [23] and $[AuCl(PPh_3)]$ [24] were prepared by literature methods; all other reagents were used as received.

4.2. Syntheses

4.2.1. Synthesis of $[N(PPh_3)_2][2\text{-}CO\text{-}2\text{-}NO\text{-}closo\text{-}2,1\text{-}CoCB_{10}H_{11}]$ (1a)

The carborane salt $[NMe_4][closo\text{-}2\text{-}CB_{10}H_{11}]$ (0.500 g, 2.43 mmol) was suspended in THF (50 ml) and $[Co(CO)_3(NO)]$ (0.50 ml, 4.25 mmol) added, followed by $[N(PPh_3)_2]Cl$ (0.1 g) and the mixture stirred for 40 h at ambient temperatures. More $[N(PPh_3)_2]Cl$ (1.40 g, 2.44 mmol) was added and stirring continued a further 1 h. Removal of volatiles in vacuo gave a brown residue, which was extracted with CH_2Cl_2 (ca. 50 ml). The extract was filtered through a Celite plug, concentrated to ca. 10 ml and applied to the top of a chromatography column. Elution first with CH_2Cl_2–petroleum ether (1:1) removed a small amount of residual $[Co(CO)_3(NO)]$ (identified by IR spectroscopy). A second, dark red–brown fraction was eluted with CH_2Cl_2–petroleum ether (3:2), containing an unstable and as yet unidentified cobalt–carborane species in low variable yields of up to 0.1 g. The main product was eluted with CH_2Cl_2–petroleum ether (3:1) as a broad brown band, which was collected and evaporated in vacuo to give dark brown microcrystals of **1a** (1.14 g).

4.2.2. Synthesis of $[N(PPh_3)_2][2\text{-}L\text{-}2\text{-}NO\text{-}closo\text{-}2,1\text{-}CoCB_{10}H_{11}]$ [$L = PPh_3$ (1b), PEt_3 (1c), $CNBu^t$ (1d)]

Compound **1a** (0.300 g, 0.38 mmol) and PPh_3 (0.105 g, 0.40 mmol) were dissolved in CH_2Cl_2 (30 ml) and the mixture cooled to −78 °C. Solid Me_3NO (0.029 g, 0.39 mmol) was added, and the solution was allowed to warm to room temperature (r.t.) and stirred for 16 h. Evaporation in vacuo gave a dark green–purple residue which was taken up in CH_2Cl_2 (5 ml) and chromatographed. Elution with CH_2Cl_2–petroleum ether (1:1) gave a small amount of $[Co(CO)_3(NO)(PPh_3)]$ [identified by IR spectroscopy (CH_2Cl_2): $\nu_{max}(CO)$ 2034 s, 1975 vs; $\nu_{max}(NO)$ 1751 s cm^{-1}] [25]. Further elution with CH_2Cl_2–THF (ca. 200:1) gave a broad, dark purple band which was collected, evaporated in vacuo and recrystallized from CH_2Cl_2–petroleum ether (−30 °C) to give **1b** (0.241 g) as dark purple prisms.

A solution of **1a** (0.150 g, 0.19 mmol) in CH_2Cl_2 (20 ml) was cooled to −78 °C and PEt_3 (29 μl, 0.20 mmol) added. The mixture gradually became purple upon warming to r.t., where it was stirred for a further 8 h. Solvent volume was reduced to ca. 5 ml and the resultant transferred to the top of a chromatography column. Elution with CH_2Cl_2 gave a broad purple band that was collected and evaporated in vacuo giving **1c** (0.136 g) as purple microcrystals.

A solution of **1a** (0.150 g, 0.19 mmol) in CH_2Cl_2 (20 ml) was cooled to −78 °C and $CNBu^t$ (22 μl, 0.19 mmol) added. The color of the solution gradually changed from brown to purple upon warming and stirring at r.t. for 8 h. Evaporation in vacuo gave a dark brown–purple residue that was dissolved in CH_2Cl_2–petroleum ether (1:1, ca. 5 ml) and chromatographed. Elution first with CH_2Cl_2–petroleum ether (1:1) removed a small quantity of $[Co(CNBu^t)(CO)_2(NO)]$, identified by IR spectroscopy (CH_2Cl_2) [$\nu_{max}(CN)$ 2169 m; $\nu_{max}(CO)$ 2043 s, 1987 vs; $\nu_{max}(NO)$ 1758 s cm^{-1}] [25]. Continued elution, using CH_2Cl_2–petroleum ether (3:1), gave a faint yellow band, identified as $[2,2,2\text{-}(CNBu^t)_3\text{-}\mathit{closo}\text{-}2,1\text{-}CoCB_{10}H_{11}]$ (**2**, up to ca. 0.01 g). Finally, with CH_2Cl_2–THF (200:1) a broad purple band was eluted, which was collected and evaporated in vacuo to give **1d** as a purple microcrystalline solid (0.114 g).

4.2.3. *Synthesis of $[2,2,2\text{-}(CNBu^t)_3\text{-}\mathit{closo}\text{-}2,1\text{-}CoCB_{10}H_{11}]$ (**2**)*

Compound **1a** (0.300 g, 0.38 mmol) in CH_2Cl_2 (20 ml) was treated with excess $CNBu^t$ (0.1 ml) and the mixture stirred for 16 h at r.t., after which the dark yellow–brown solution was evaporated in vacuo. Chromatographic work-up as for **1d** above gave, in addition to small amounts of $[Co(CNBu^t)(CO)_2(NO)]$ and **1d** (ca. 0.02 g), compound **2** as a yellow microcrystalline solid (0.115 g).

4.2.4. *Synthesis of $[2\text{-}NO\text{-}2\text{-}PEt_3\text{-}7\text{-}L\text{-}\mathit{closo}\text{-}2,1\text{-}CoCB_{10}H_{10}]$ [L = $O(CH_2)_4$ (**3a**), NCMe (**3b**), N(Me)=C(H)Me (**3c**)]*

Compound **1c** (0.100 g, 0.11 mmol) was dissolved in CH_2Cl_2–THF (10:1, 25 ml) and CF_3SO_3Me (0.1 ml) added. The resultant mixture was stirred for 2 h and then evaporated in vacuo. The purple residue was dissolved in the minimum volume (ca. 2 ml) of CH_2Cl_2 and transferred to the top of a chromatography column. Elution with CH_2Cl_2–petroleum ether (7:3) gave a broad purple band that was collected and evaporated in vacuo. The resultant mixture was further purified by preparative TLC, eluting with the same solvent mixture, and then recrystallization (CH_2Cl_2–petroleum ether, −30 °C), yielding purple microcrystals of **3a** (0.018 g).

Similarly, compound **1c** (0.100 g, 0.11 mmol) with CF_3SO_3Me (0.1 ml) in CH_2Cl_2–NCMe (10:1, 25 ml), after column chromatography using CH_2Cl_2–petroleum ether (7:3) gave crude **3b** as a purple solid. Further purification of the latter by preparative TLC, using the same solvent mixture, afforded two purple bands that were collected and recrystallized (CH_2Cl_2–petroleum ether, −30 °C) to give **3b** (R_F 0.75, 0.015 g) and a small quantity of **3c** (R_F 0.85, ca. 0.001 g) as purple microcrystals.

4.2.5. *Synthesis of bimetallic compounds*

To a solution of compound **1a** (0.150 g, 0.19 mmol) in THF (25 ml) was added solid $[CuCl(PPh_3)]_4$ (0.069 g, 0.05 mmol) and $Tl[PF_6]$ (0.067 g, 0.19 mmol). The mixture was stirred for 6 h and evaporated in vacuo. The residue was extracted with CH_2Cl_2, and the extract was filtered through a Celite plug and then concentrated to approximately 2 ml and subjected to column chromatography. Elution with CH_2Cl_2–petroleum ether (3:2) gave two closely-spaced fractions: first a brown band, which upon evaporation in vacuo gave brown microcrystalline $[2,7,11\text{-}\{Cu(PPh_3)\}\text{-}7,11\text{-}(\mu\text{-}H)_2\text{-}2\text{-}CO\text{-}2\text{-}NO\text{-}\mathit{closo}\text{-}2,1\text{-}CoCB_{10}H_9]$ (**4a**, 0.043 g), and then a purple band which was evaporated in vacuo yielding purple microcrystals of $[2,7,11\text{-}\{Cu(PPh_3)\}\text{-}7,11\text{-}(\mu\text{-}H)_2\text{-}2\text{-}NO\text{-}2\text{-}PPh_3\text{-}\mathit{closo}\text{-}2,1\text{-}CoCB_{10}H_9]$ (**4b**, 0.029 g). The first fraction so separated was found to be contaminated with a little of **4b**. However, whereas **4b** could be purified by crystallization (CH_2Cl_2–petroleum ether, −30 °C), compound **4a** proved to be very unstable and further attempted purification only gave **4b**.

To the compounds **1b** (0.050 g, 0.05 mmol), $[CuCl(PPh_3)]_4$ (0.025 g, 0.02 mmol) and $Tl[PF_6]$ (0.018 g, 0.05 mmol) was added THF (25 ml) and the mixture stirred for 16 h. The more volatile components were removed in vacuo and the residue extracted with CH_2Cl_2. The filtered extract was concentrated by evaporation in vacuo to ca. 2 ml and chromatographed. Elution with CH_2Cl_2–petroleum ether (3:2) gave a purple band, which upon evaporation in vacuo, gave **4b** (0.036 g) as purple microcrystals.

Similarly, compound **1b** (0.075 g, 0.07 mmol), $Ag[BF_4]$ (0.015 g, 0.08 mmol) and PPh_3 (0.020 g, 0.08 mmol) gave purple $[2,7\text{-}\{Ag(PPh_3)\}\text{-}7\text{-}\mu\text{-}H\text{-}2\text{-}NO\text{-}2\text{-}PPh_3\text{-}\mathit{closo}\text{-}2,1\text{-}CoCB_{10}H_{10}]$ (**5**, 0.049 g).

By a comparable procedure, compound **1b** (0.075 g, 0.07 mmol), $[AuCl(PPh_3)]$ (0.038 g, 0.08 mmol) and $Tl[PF_6]$ (0.027 g, 0.08 mmol) afforded brown–purple $[2\text{-}\{Au(PPh_3)\}\text{-}2\text{-}NO\text{-}2\text{-}PPh_3\text{-}\mathit{closo}\text{-}2,1\text{-}CoCB_{10}H_{11}]$ (**6**, 0.007 g).

4.3. *Crystallography*

Experimental data for compounds **1a** and **4b** are recorded in Table 4. Diffracted intensities were collected on an Enraf-Nonius CAD4 diffractometer operating in the ω–2θ scan mode, using graphite-monochromated Mo Kα X-radiation ($\lambda = 0.71073$ Å). Final unit cell dimensions were determined from the setting angles of 25 accurately centered reflections. Intensity data were corrected for Lorentz and polarization effects. A semi-empirical absorption correction (ψ scans) was applied for **1a**.

Table 4
Crystal data for **1a** and **4b**·OEt_2

	1a	**4b**·OEt_2
Empirical formula	$C_{38}H_{41}B_{10}CoN_2O_2P_2$	$C_{37}H_{41}B_{10}CoCuNOP_2\cdot C_4H_{10}O$
M_r	786.70	882.34
Crystal color, habit	dark red, acicular needles	purple, cubes
Crystal size (mm)	0.64 × 0.20 × 0.13	0.10 × 0.10 × 0.10
Crystal system	monoclinic	triclinic
Space group	$P2_1/c$	$P\bar{1}$
a (Å)	14.610(2)	10.590(3)
b (Å)	18.375(3)	12.172(2)
c (Å)	15.432(2)	19.016(5)
α (°)	90	71.43(2)
β (°)	101.330(12)	85.40(2)
γ (°)	90	68.72(2)
U (Å^3)	4062.2(10)	2163.4(9)
Z	4	2
D_{calc} (Mg m^{-3})	1.286	1.355
μ (mm^{-1})	0.538	0.986
Temperature (K)	173(2)	293(2)
Reflections collected	5358	3309
Independent reflections	5124 ($R_{int} = 0.0646$)	3168 ($R_{int} = 0.0360$)
Observed reflections [$F > 4\sigma(F)$]	3589	2743
Final R indices [a]	$R_1 = 0.0555$, $wR_2 = 0.1548$	$R_1 = 0.0638$, $wR_2 = 0.1629$
Goodness-of-fit on F^2	1.058	1.444
Largest difference peak and hole (e Å^{-3})	0.321 and −0.465	0.699 and −0.915

[a] $R_1 = \Sigma||F_o|-|F_c||/\Sigma|F_o|$ for $F_o > 4\sigma(F_o)$; $wR_2 = [\Sigma\{w(F_o{}^2-F_c{}^2)^2\}/\Sigma\, w(F_o{}^2)^2]^{1/2}$ for all data.

Both structures were solved with conventional direct methods and refined by full-matrix least-squares on all F^2 data using SHELXTL version 5.03 and SHELXL-97 [26,27]. For compound **1a**, all non-hydrogen atoms were assigned anisotropic thermal displacement parameters. The locations of the cage-carbon atoms were verified by examination of the appropriate internuclear distances in conjunction with the magnitudes of their isotropic thermal displacement parameters. The cobalt-bound CO and NO ligands in **1a** were similarly differentiated. Crystals of **4b** were small and diffracted poorly. In an attempt to maintain a respectable data: parameter ratio for that determination, the carbon atoms comprising the phenyl rings on both triphenylphosphine groups were refined with equivalent anisotropic thermal parameters using the SHELX-97 EADP card; the boron atoms in the carborane cage were refined similarly. All hydrogens in both compounds, including the agostic B–H⇀Cu hydrogens H(3) and H(4) in **4b**, were included in calculated positions and refined with fixed isotropic thermal parameters, $U_{iso}(H) = 1.2 \times U_{iso}(\text{parent})$.

Compound **4b** co-crystallized with one fully-ordered molecule of diethyl ether. The analogous carbons on each ethyl chain were assigned equivalent anisotropic thermal parameters using the SHELXL-97 EADP card; hydrogen atoms were included in calculated positions and with fixed isotropic thermal parameters, $U_{iso}(H) = 1.2 \times U_{iso}(\text{parent})$ or $1.5 \times U_{iso}(\text{parent})$ for CH_2 and CH_3 groups, respectively.

5. Supplementary material

Full crystallographic data in CIF format have been deposited with The Director, CCDC, 12 Union Road, Cambridge, CB2 1EZ, UK (fax: +44-1223-366033; e-mail: deposit@ccdc.cam.ac.uk or www: http://www.ccdc.cam.ac.uk) and are available on request, quoting deposition numbers 188504 or 188505 for compounds **1a** and **4b**, respectively.

Acknowledgements

We thank the Robert A. Welch Foundation for support (Grant AA-1201).

References

[1] M.F. Hawthorne, D.C. Young, P.A. Wegner, J. Am. Chem. Soc. 87 (1965) 1818.
[2] (a) D.E. Hyatt, J.L. Little, J.T. Moran, F.R. Scholer, L.J. Todd, J. Am. Chem. Soc. 89 (1967) 3342;
(b) W.H. Knoth, J. Am. Chem. Soc. 89 (1967) 3342.
[3] C. Janiak, H. Schumann, Adv. Organomet. Chem. 33 (1991) 291.
[4] See, for example, together with references therein: (a) R.N. Grimes, in: G. Wilkinson, E.W. Abel, F.G.A. Stone (eds.), Comprehensive Organometallic Chemistry, vol. 1, Pergamon Press, Oxford, 1982, sect. 5.5; (b) R.N. Grimes, in: E.W. Abel, F.G.A. Stone, G. Wilkinson (Eds.), Comprehensive Organometallic Chemistry II, vol. 1, Pergamon Press, Oxford, 1995, chapter 9; (c) R.N. Grimes, Coord. Chem. Rev. 200–202 (2000) 773.
[5] S.A. Batten, J.C. Jeffrey, P.L. Jones, D.F. Mullica, M.D. Rudd, E.L. Sappenfield, F.G.A. Stone, A. Wolf, Inorg. Chem. 36 (1997) 2570.
[6] I. Blandford, J.C. Jeffrey, P.A. Jelliss, F.G.A. Stone, Organometallics 17 (1998) 1402.
[7] J.C. Jeffrey, P.A. Jelliss, L.H. Rees, F.G.A. Stone, Organometallics 17 (1998) 2258.
[8] D.D. Ellis, A. Franken, P.A. Jelliss, F.G.A. Stone, P.-Y. Yu, Organometallics 19 (2000) 1993.
[9] D.D. Ellis, A. Franken, P.A. Jelliss, F.G.A. Stone, P.-Y. Yu, J. Chem. Soc., Dalton Trans. (2000) 2509.
[10] D.D. Ellis, A. Franken, T.D. McGrath, F.G.A. Stone, J. Organomet. Chem. 614–615 (2000) 208.
[11] A. Franken, S. Du, P.A. Jelliss, J.A. Kautz, F.G.A. Stone, Organometallics 20 (2001) 1597.
[12] S. Du, A. Franken, P.A. Jelliss, J.A. Kautz, F.G.A. Stone, P.-Y. Yu, J. Chem. Soc., Dalton Trans. (2001) 1846.
[13] S. Du, J.A. Kautz, T.D. McGrath, F.G.A. Stone, J. Chem. Soc., Dalton Trans. (2001) 2791.

[14] J.A. Kautz, T.D. McGrath, F.G.A. Stone, in: Abstracts, Eighth Biennial Boron Americas Conference, Death Valley, CA, USA, 2002, p. 73, poster P17.

[15] S.L. Hendershot, J.C. Jeffrey, P.A. Jelliss, D.F. Mullica, E.L. Sappenfield, F.G.A. Stone, Inorg. Chem. 35 (1996) 6561.

[16] (a) J.C. Jeffery, F.G.A. Stone, I. Topaloglu, J. Organomet. Chem. 451 (1993) 205;
(b) S.J. Dossett, S. Li, F.G.A. Stone, Polyhedron 13 (1994) 1773;
(c) D.D. Ellis, P.A. Jelliss, F.G.A. Stone, Chem. Commun. (1999) 2385.;
(d) T.E. Bitterwolf, W.B. Scallorn, C.A. Weiss, P.A. Jelliss, Organometallics 21 (2002) 1856.

[17] F.G.A. Stone, J. Organomet. Chem. 100 (1975) 257 (and references therein).

[18] W.E. Carroll, M. Green, F.G.A. Stone, A.J. Welch, J. Chem. Soc., Dalton Trans. (1975) 2263.

[19] D.M.P. Mingos, M.I. Forsyth, A.J. Welch, J. Chem. Soc., Dalton Trans. (1978) 1363.

[20] For example, M.F. Hawthorne, L.F. Warren Jr., K.P. Callahan, N.F. Travers, J. Am. Chem. Soc. 93 (1971) 2407; see also refs [8,11–13].

[21] S. Du, J.A. Kautz, T.D. McGrath, F.G.A. Stone, Inorg. Chem. 40 (2001) 6563.

[22] D.E. Hyatt, F.R. Scholer, L.J. Todd, J.L. Warner, Inorg. Chem. 6 (1967) 2229.

[23] F.H. Jardine, J. Rule, G.A. Vohra, J. Chem. Soc. A (1970) 238.

[24] M.I. Bruce, B.K. Nicholson, O. Bin Shawkataly, Inorg. Synth. 26 (1989) 325.

[25] R.D.W. Kemmitt, D.R. Russell, in: G. Wilkinson, E.W. Abel, F.G.A. Stone (Eds.), Comprehensive Organometallic Chemistry, vol. 5 (sect. 34, and references therein), Pergamon Press, Oxford, 1982, pp. 24–29.

[26] SHELXTL version 5.03, Bruker AXS, Madison WI, 1997.

[27] G.M. Sheldrick, SHELXL-97, University of Göttingen, Germany, 1997.